AD-A086 420 MCDONNELL DOUGLAS ASTRONAUTICS CO HUNTINGTON BEACH CA F/G 4/1
PLASMA FIELD STUDIES DURING MAGNETIC DISTURBANCES.(U)
JUN 80 W P OLSON, K A PFITZER, S J SCOTTI N00014-79-C-0791
UNCLASSIFIED NL

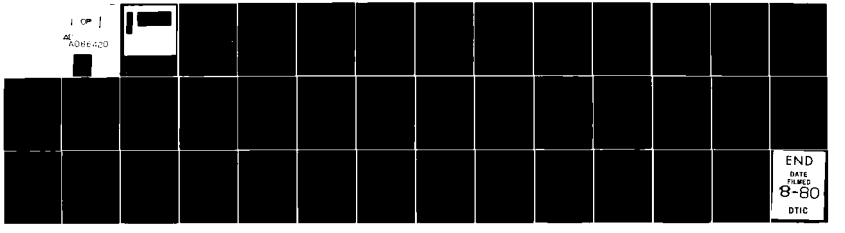

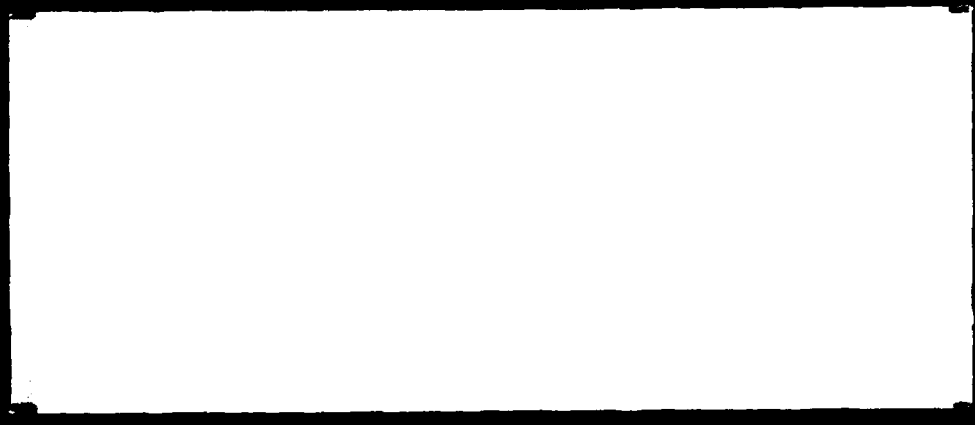

MCDONNELL DOUGLAS ASTRONAUTICS COMPANY

MCDONNELL DOUGLAS CORPORATION

MCDONNELL DOUGLAS

PLASMA FIELD STUDIES DURING MAGNETIC DISTURBANCES

June 1980

Final Report for Contract
N00014-79-C-0791 Sponsored by the
Office of Naval Research

Principal Investigator: W. P. Olson

Co-Investigators: K. A. Pfitzer
S. J. Scotti

MCDONNELL DOUGLAS ASTRONAUTICS COMPANY-WEST
5301 Bolsa Avenue, Huntington Beach, CA 92647

SECURITY CLASSIFICATION OF THIS PAGE (When Data Entered)

REPORT DOCUMENTATION PAGE		READ INSTRUCTIONS BEFORE COMPLETING FORM
1. REPORT NUMBER	2. GOVT ACCESSION NO.	3. RECIPIENT'S CATALOG NUMBER
4. TITLE (and Subtitle) PLASMA FIELD STUDIES DURING MAGNETIC DISTURBANCES		5. TYPE OF REPORT & PERIOD COVERED Final 8/79 - 6/80 6. PERFORMING ORG. REPORT NUMBER
7. AUTHOR(s) W. P. Olson K. A. Pfitzer S. J. Scotti		8. CONTRACT OR GRANT NUMBER(s) N00014-79-C-0791
9. PERFORMING ORGANIZATION NAME AND ADDRESS McDonnell Douglas Astronautics Company 5201 Bolsa Avenue Huntington Beach, CA 92647		10. PROGRAM ELEMENT, PROJECT, TASK AREA & WORK UNIT NUMBERS
11. CONTROLLING OFFICE NAME AND ADDRESS Office of Naval Research Ballston Center Tower #1 800 N. Quinny, Arlington, VA 02217		12. REPORT DATE 30 Jun 1980 13. NUMBER OF PAGES 121
14. MONITORING AGENCY NAME & ADDRESS(if different from Controlling Office)		15. SECURITY CLASS. (of this report) Unclassified 15a. DECLASSIFICATION DOWNGRADING SCHEDULE

16. DISTRIBUTION STATEMENT (of this Report)

Approved for public release, distribution unlimited.

17. DISTRIBUTION STATEMENT (of the abstract entered in Block 20, if different from Report)

18. SUPPLEMENTARY NOTES

Tech., others

19. KEY WORDS (Continue on reverse side if necessary and identify by block number)

Magnetosphere, Quantitative Models, Magnetic Field, Electric Field, Substorm.

20. ABSTRACT (Continue on reverse side if necessary and identify by block number)

This work summarizes the work performed during the contract period. The goal was the development of quantitative disturbed-time magnetic and electric field in the magnetosphere.

The July 29, 1980 event was the model disturbance used to develop a realistic magnetic and electric field model for a disturbed period.

DD FORM 1 JAN 73 1473 EDITION OF 1 NOV 65 IS OBSOLETE

3/1210

SECURITY CLASSIFICATION OF THIS PAGE (When Data Entered)

TABLE OF CONTENTS

Section 1.0
INTRODUCTION AND SUMMARY

The purpose of our work this past year has been to extend our study of induced electric fields in the magnetosphere. Earlier we examined the induced electric fields produced by the response of the magnetosphere to the daily wobble of the earth's dipole axis. It was determined that this field, which is always present, is large enough to influence charged particles in the magnetosphere.

It is known that much larger time variations in the magnetospheric magnetic field occur and that their associated electric fields are also larger. In our study of storm time electric fields we have restricted ourselves to the symmetric case (solar wind incident perpendicular to the dipole axis.) This permits the more economical study of "equatorial" charged particles. (This was not possible in our earlier work on the wobbling dipole.) We found the magnetic contributions individually for the magnetopause, ring, and tail current systems together with their associated vector magnetic potentials. With these tools it is also possible to determine the appropriate induced electric fields. Our work on the storm time induced electric field was the main emphasis of this years effort.
Several conclusions from our study discussed in detail in the report are listed here:

- At the Coordinated Data Analysis Workshop on the July 29, 1977 substorm we were able to quantitatively model the induced electric field. We were also able to qualitatively demonstrate that this field was capable of producing the acceleration of charged particles in the magnetosphere observed during the event.
- The ionosphere, acting through its static electric field, exerts considerable influence on the magetosphere. The work we wanted to do comparing STARE data with satellite electric field measurements was abandoned because of the questionable quality of the existing satellite electric field data.

- The problem of excessive computer time on charged particle energization studies remains. This has led us to study the possible use of Euler potentials.

- We have correctly modeled induced electric fields in the magnetosphere and understand the procedures required for finding the induced field for any time varying magnetospheric magnetic field.

- The remaining important magnetospheric electric field, the so-called cross-tail field, has not yet been quantitively characterized. We feel that we understand how this field is generated and its association with the plasma sheet and the cross-tail currents.

The remainder of the report is structured as follows. First a general discussion of electric fields, taken from the proposal, is presented. This is followed by a discussion of our present ability to represent the time varying disturbed magnetospheric magnetic field and a discussion of the boundary value problem used to determine the total magnetospheric electric field. The report also contains a description of Euler potentials as they might be applied to the study of time varying magnetic fields and their associated induced electric fields.

Section 2.0
COMMENTS ON THE MAGNETOSPHERIC ELECTRIC FIELD

The magnetosphere contains many regions in which energetic particles are trapped. Several detailed explanations have been given for the existence of the very high energy Van Allen radiation. The remaining energetic particle populations, however, must be explained in terms of the interaction of their source regions, the solar wind and the upper atmosphere, with the geomagnetic field. The solar wind has particle energies on the order of 1 keV while the energetic particle populations within the magnetosphere have energies which range from several keV to several hundred keV. It is therefore necessary to explain the energization of these particles in terms of "local" acceleration mechanisms. That is, the energization of these particles must take place within the magnetosphere or in the shock and magnetosheath regions which surround it. There are only two ways in which charged particles can be accelerated: either by time varying magnetic fields or the presence of electrostatic fields.

Generically there are two kinds of electric fields: electrostatic fields which result from charge separation over a region of space, and time varying magnetic fields which have associated induced electric fields.

In the earth's magnetosphere several electric fields have been postulated to explain observed plasma phenomena. The electric fields associated with the rotation of the earth are used to explain the corotation of the plasma which populates the plasmasphere. A "convection" electric field arising from some unknown viscous interaction between the magnetosphere and the solar wind has been postulated to explain gross plasma motions in the magnetosphere. More recently electric fields in the ionosphere-magnetosphere system have been suggested to explain the existence of currents flowing along magnetic field lines. Thus, the electric fields that have been discussed in the literature to date have been linked with specific observations in the magnetosphere but have not typically addressed the general question of particle acceleration and energization.

It is useful then to consider what we know quantitatively about the existence of electric fields in the magnetosphere. It turns out that little is known concerning the electrostatic fields caused by charge separation. The subject of induced electric fields has also received little attention to date. However, the source of an induced electric field must be a time varying magnetic field. Considerable work has recently been done on the nature of time varying magnetic fields in the magnetosphere. Thus, the source of at least some induced electric fields is understood quantitatively.

From the point of view of particle energization the induced electric field is more interesting than the electrostatic field since it is not conservative and particles moving in it can be accelerated and energized even when they move over a closed path.

In order to quantitatively represent the electric field produced during disturbed magnetic conditions, it is first necessary to have a quantitative representation of the source of that field -- the time varying magnetospheric magnetic field. We recently have developed the tools for generally representing the total magnetospheric magnetic field during arbitrarily changing storm conditions. To do this, it was necessary to represent the contribution to the total magnetic field produced by each of the three major current systems flowing through the magnetosphere. In the past only the total magnetic field was considered. However, during magnetically disturbed periods each of these current systems vary in strength and location independently of the others. It was, therefore, necessary to redetermine the contributions from each of these three current systems separately with the appropriate spacing of the points throughout the magnetosphere where the magnetic field would be determined. Special attention was given to the nose and distant tail regions.

The procedure then was as follows. The magnetic field was redetermined for each of the three current systems separately with appropriate spacing of the points throughout the magnetosphere. Each component of the magnetic field, $\bar{B}$ was determined for the three current systems to obtain a total of nine separate series expansions. The form of the series was chosen to maximize the goodness

of the fit between the input raw data and the computed least squares best fit. The average errors over all nine components distributed throughout the magnetosphere is on the order of 8 percent. Most of the large percent errors occurred farther down the tail, where the total actual field is typically smaller than 1 gamma. Thus, the absolute errors are not large over most of the magnetosphere (less than 2 gamma).

Using these series expansions to represent individually the contributions to the total magnetic field from the three major magnetospheric current systems, it is possible to quantitatively determine the topology of the magnetospheric magnetic field during disturbed conditions. For these expansions to be useful, it is required that a "template" of the storm be obtained. The template (which takes the form of a driver program in the computer deck) provides information concerning the variation with time in the strengths and locations of these three current systems.

Section 3.0
EVENT SPECIFIC STORM MODELS

The first "template" chosen for this work was the July 29, 1978 event which is comprised of a well documented set of substorms. The dependence of each of the three major magnetospheric current systems on changes in solar wind and interplanetary field parameters was determined. This was the first event specific model of the magnetospheric magnetic and electric fields to be developed. The temporal variations in the magnetic field provided the "template" needed for the calculation of the induced electric field. The procedures for quantitatively determining $\overline{B}$ and $\overline{E}$ are described in detail below.

3.1 CURRENT SYSTEMS AND MAGNETIC FIELDS

3.1.1 The Magnetopause Currents

The strength and size of the magnetopause currents for the July 29 event are determined classically using a pressure balance equation which relates the kinetic pressure of the solar wind to the magnetic energy density (or pressure) of the magnetic field inside the magnetopause. In Figures 1 and 2, the velocity and density of the solar wind are shown throughout the event epoch beginning at noon on July 28. Notice that most of the variability in the solar wind pressure is caused by changes in the density of the solar wind. (The solar wind velocity seldom drops below 250 kilometers/second and has only rarely been observed above 1000 kilometers/second.) The pressure balance formalism leads directly to a standoff distance for the magnetopause when the standard assumption for the magnetospheric magnetic field is made (see Figure 3). The total magnetic field just inside the magnetopause is twice the value of the geomagnetic dipole field at that point. Note in Figure 3 that it is just after midnight that the density of the solar wind increases abruptly. At this time the magnetopause moves in abruptly - this may be considered as the sudden commencement phase of a magnetic storm. However, it is seen subsequently that the magnetosphere will respond several different ways

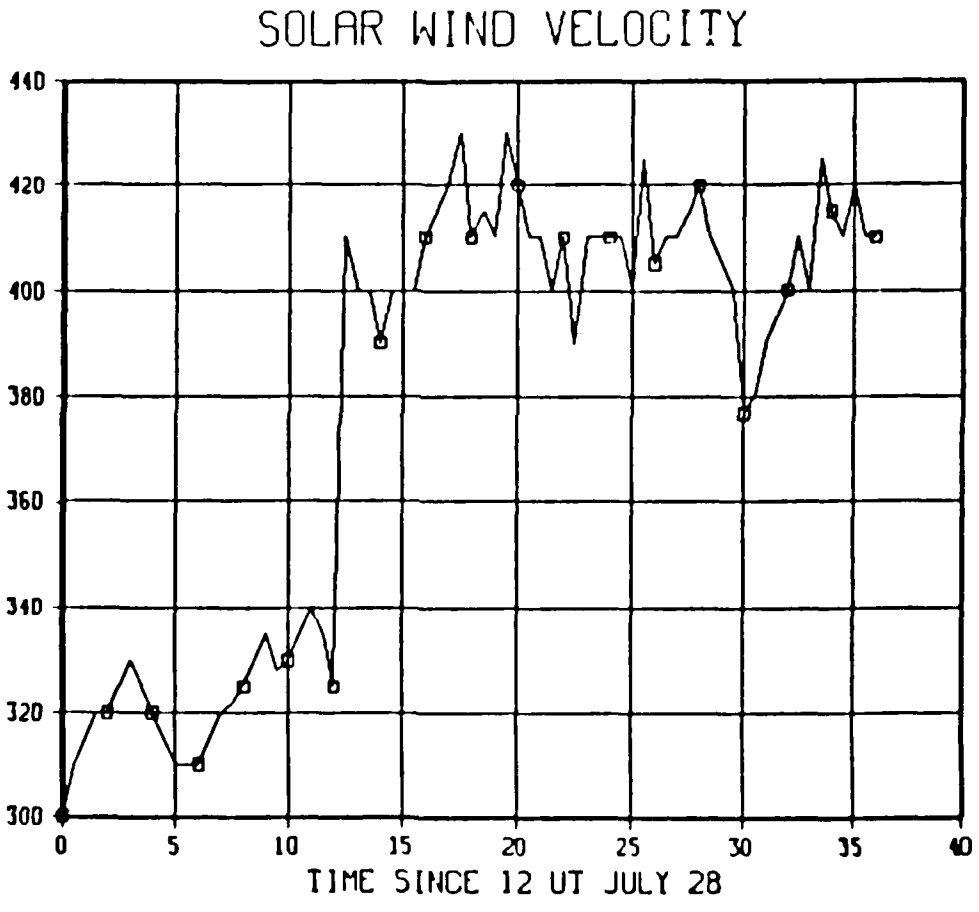

Figure 1. Solar Wind Velocity

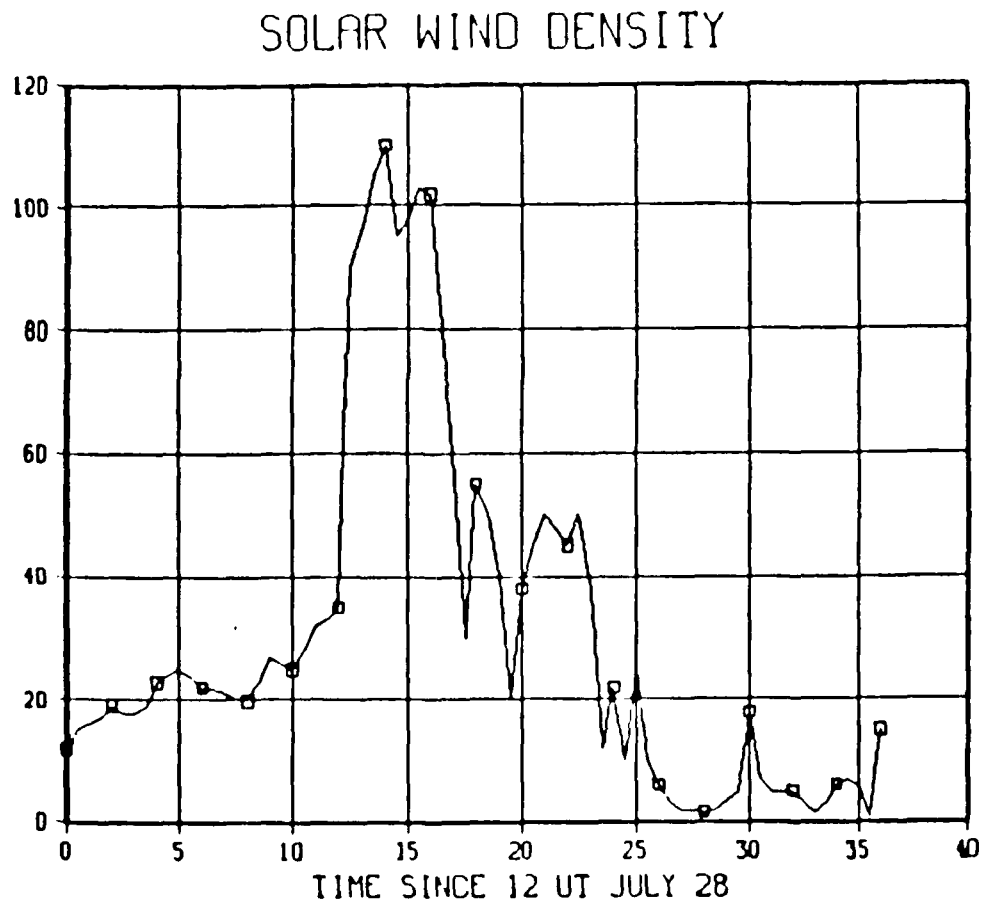

Figure 2. Solar Wind Density

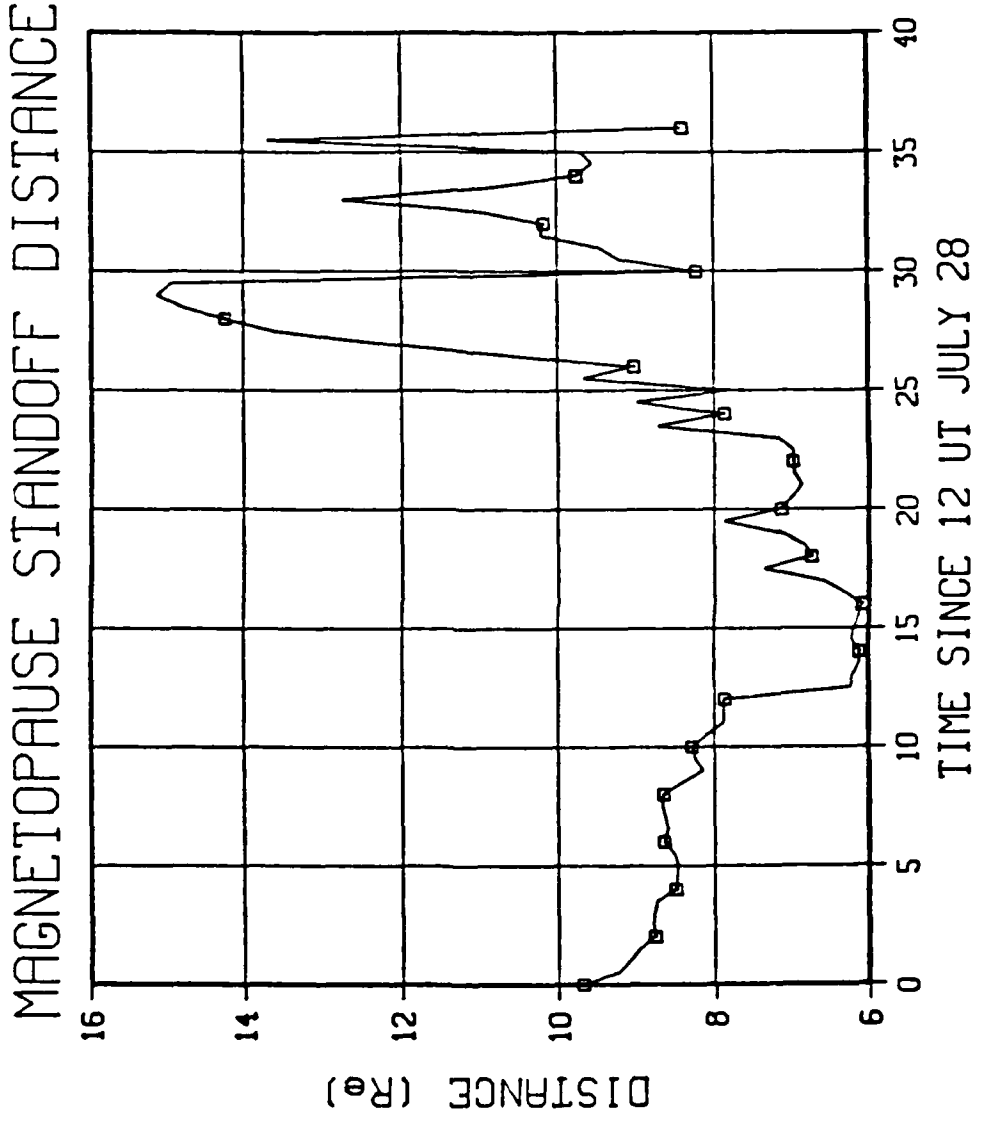

Figure 3. Magnetopause Standoff Distance

during this complex event. It is noted also that late during the event the solar wind density becomes quite low and the magnetopause relaxes outward far beyond its normal position.

The pressure balance formalism also relates the strength of the magnetopause currents and the size of the magnetopause directly to the solar wind pressure. Thus, the strength of the magnetopause currents can be obtained from a knowledge of solar wind velocity and density. The strength of the currents is shown in Figure 4. They have been normalized such that a relative current strength of 1 corresponds to a stand off distance of 10.5 R_e (earth radii). The range in the strength of the magnetopause currents throughout the event varies by over a factor of 8.

3.1.2 The Ring Current

Since this analysis was not done by computers in real time, it was possible to use ground-based magnetic indices in the analysis. Traditionally, Dst, measured at mid-latitudes is considered best for representing variations in the strength of the ring current. The variability in this magnetic index throughout the event is shown in Figure 5. Note, however, that Dst contains a sudden jump near midnight. This feature is certainly caused by compression of the magnetopause, not from an instant response of the ring current to the solar wind. We therefore were led during the Workshop to define a modified Dst in which an attempt was made to remove the contribution of the magnetopause current systems to the magnetic field recorded at the ground and used to construct the Dst index. (This could be done because the strength of the magnetopause currents had already been determined using pressure balance.) The modified values of Dst are shown in Figure 6. Note that this modified parameter exhibits no sudden commencement, an indication that the magnetopause currents have been correctly deleted. The modified Dst index was then used directly to describe the strength of the ring currents. The time variation in the ring current throughout the event is shown in Figure 7. The ring current strength varies by a factor of over 3 throughout the event. It appears to be enhanced through the first 6 hours of July 29 in association with several strong substorms. It then decays gradually through the rest of the day with some interruption due to subsequent substorm injected particles.

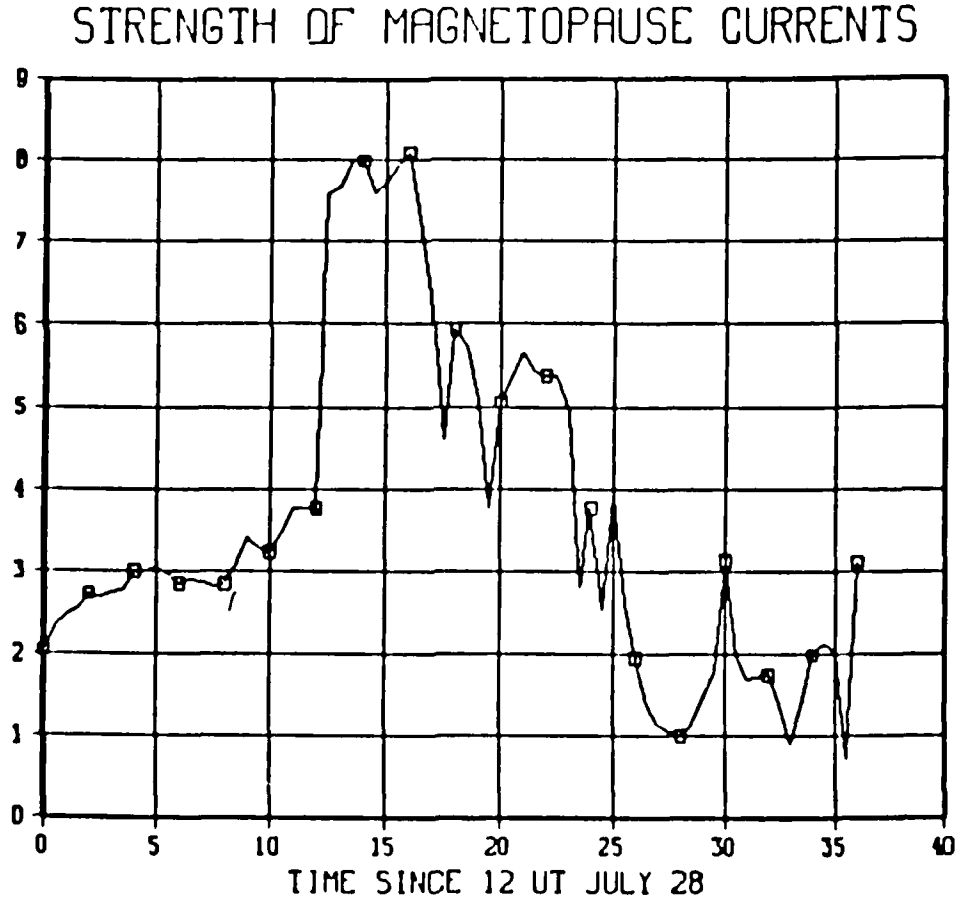

Figure 4. Strength of Magnetopause Currents

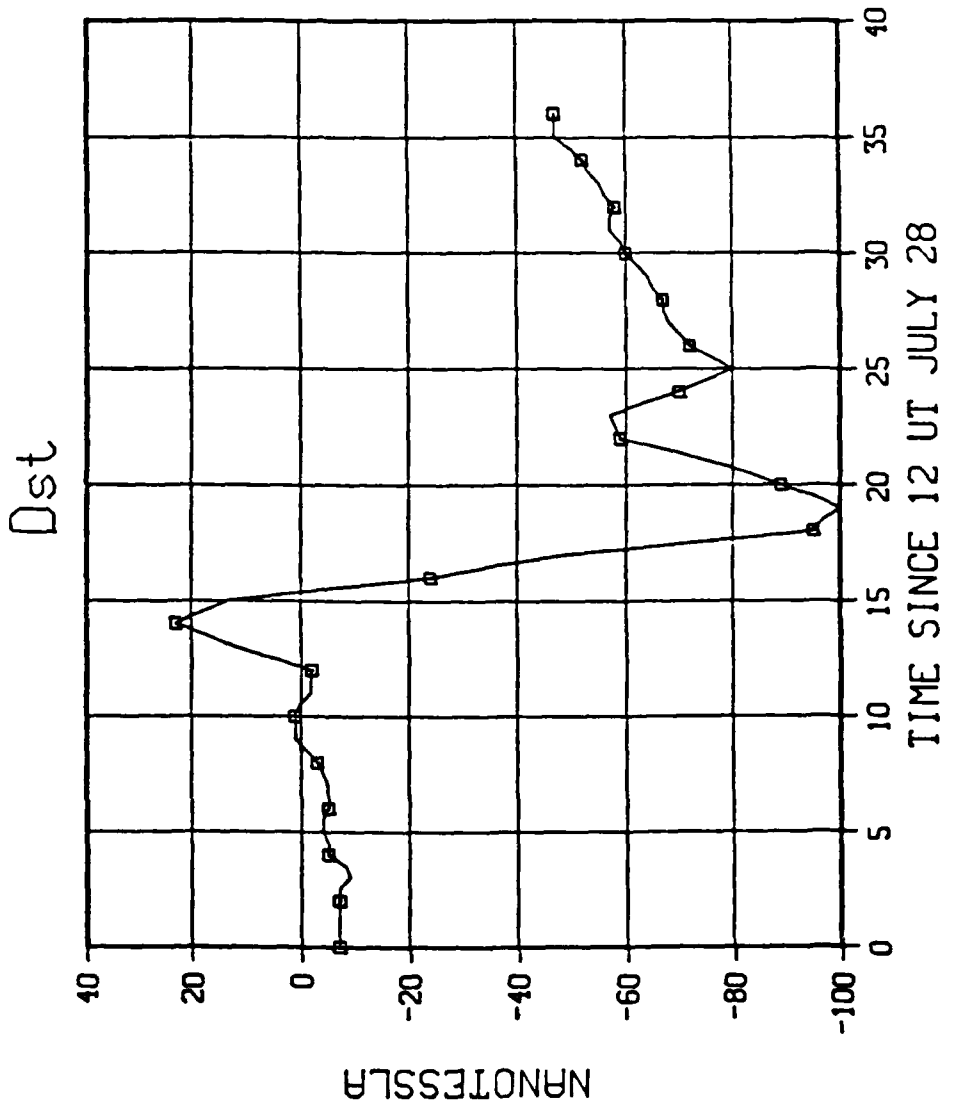
Dst
NANOTESSLA
40
20
0
-20
-40
-60
-80
-100
0
5
10
15
20
25
30
35
40
TIME SINCE 12 UT JULY 28

Figure 5. Dst

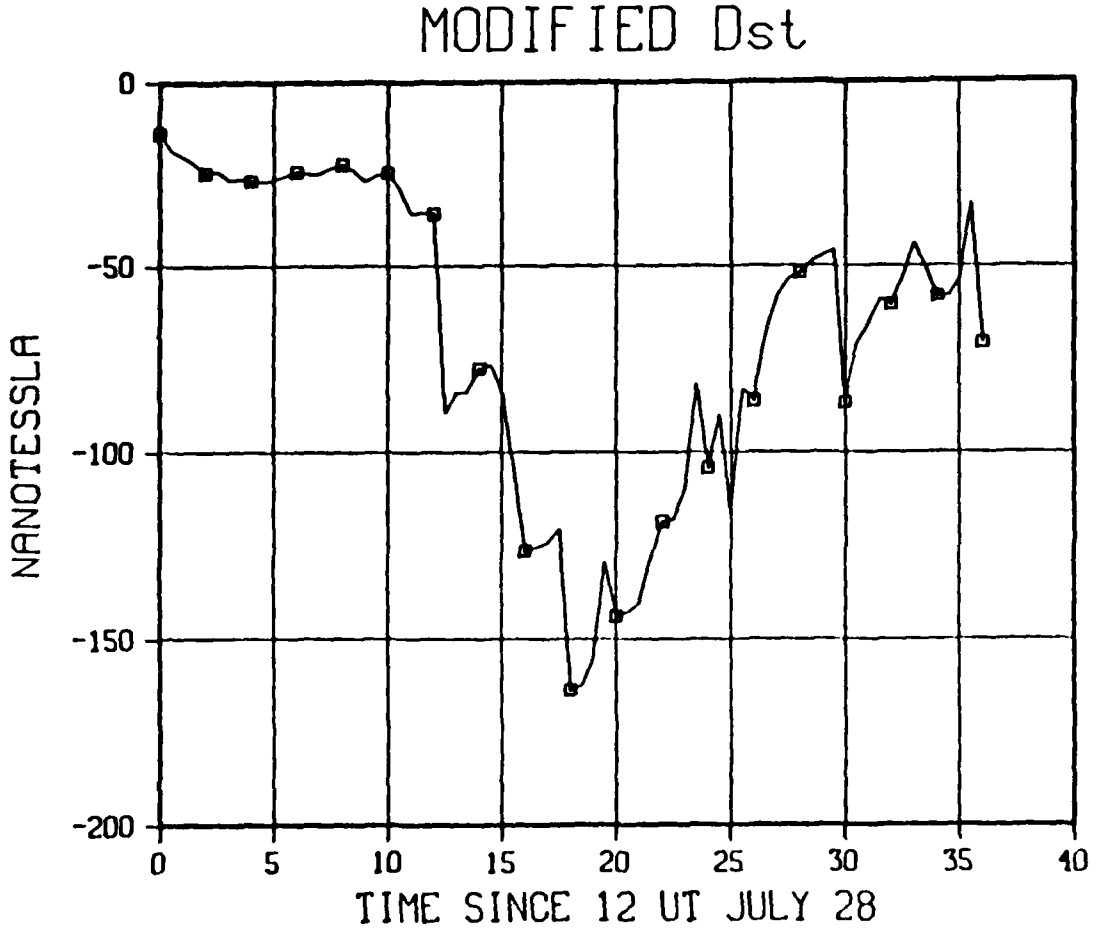

Figure 6. Modified Dst

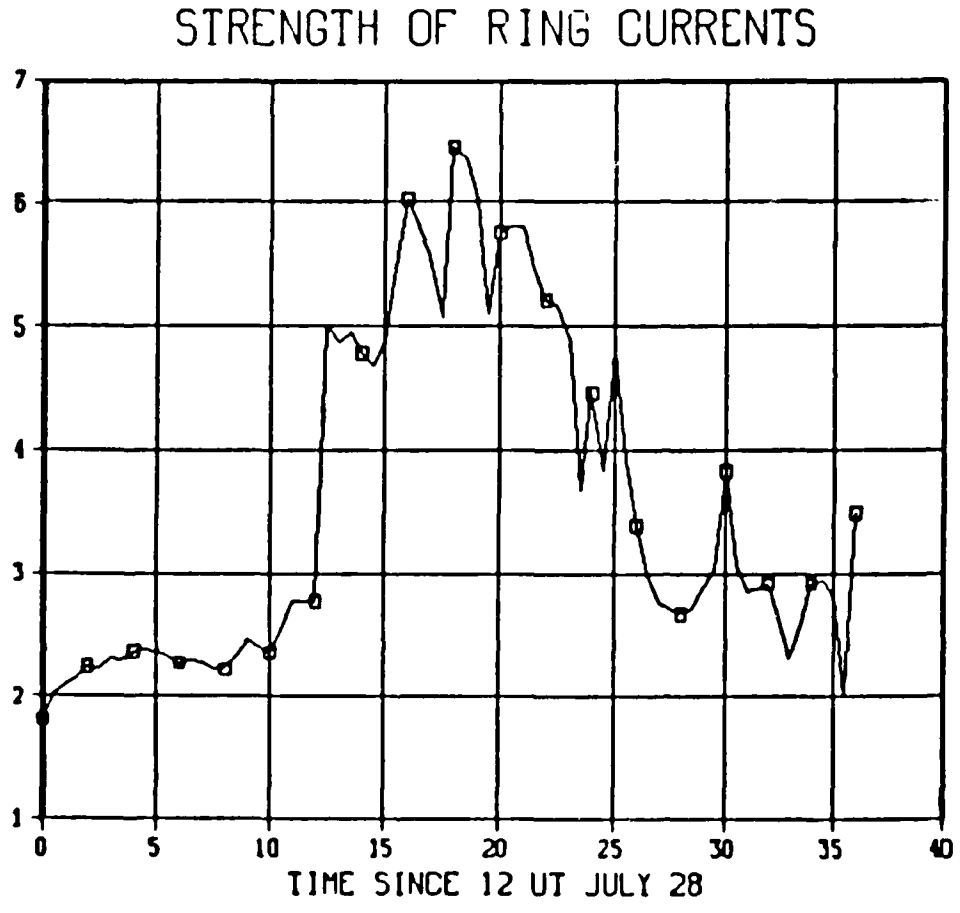

Figure 7. Strength of Ring Currents

3.1.3 The Tail Current

In the zero order model provided ahead of the meeting, the tail currents were tied directly to the magnetopause currents for want of a better procedure. During the meeting discussions with several participants indicated that it would be worthwhile trying to relate the strength of the tail current to some parameter that provided a measure of the electromagnetic energy input by the solar wind into the magnetosphere. For that purpose we used the so-called epsilon index which multiplies the Poynting vector of the interplanetary electromagnetic field (as observed in a magnetospheric reference system) by a geometry factor which attempts to represent the cross section of the magnetosphere to this energy input. In order to use this parameter, it was necessary to develop a threshold procedure since although epsilon can be zero, it is believed that the tail currents are always present. The strength of the tail currents as based on this parameter is shown in Figure 8 as it varies through the event.

3.1.4 Field Topology

The final model developed at the meeting was used to produce several plots of magnetic field topology and other magnetic field features of interest to the Workshop participants. In Figures 9 through 12, the field topology in the noon-midnight meridian plane is shown at four times through the event. However, the variability of the fields between these times was, indeed, large. They are shown here as representative of the different states of the magnetospheric magnetic field. One can easily see the compression of the magnetosphere early in the event and the effect of the increased tail current late in the event. (The divergence of the tail field lines in Figure 10 is an artifact of the model.) Changes in the field geometry are most appreciable in the tail region and, in fact, in Figure 12 if more lines were drawn it would be seen that a neutral point is in evidence in the near-earth magnetosphere.

In Figure 13, model data are compared with observations at the orbit of the geosynchronous satellite GOES 1. It is seen that the H and the D components agree reasonably well, whereas the V component which gives a measure of the tail-like nature of the field observed at the satellite suggests that the field is more tail-like than than the model predicts. The smooth lines shown in Figure 13 show the data from our quiet time model. Note that some of the

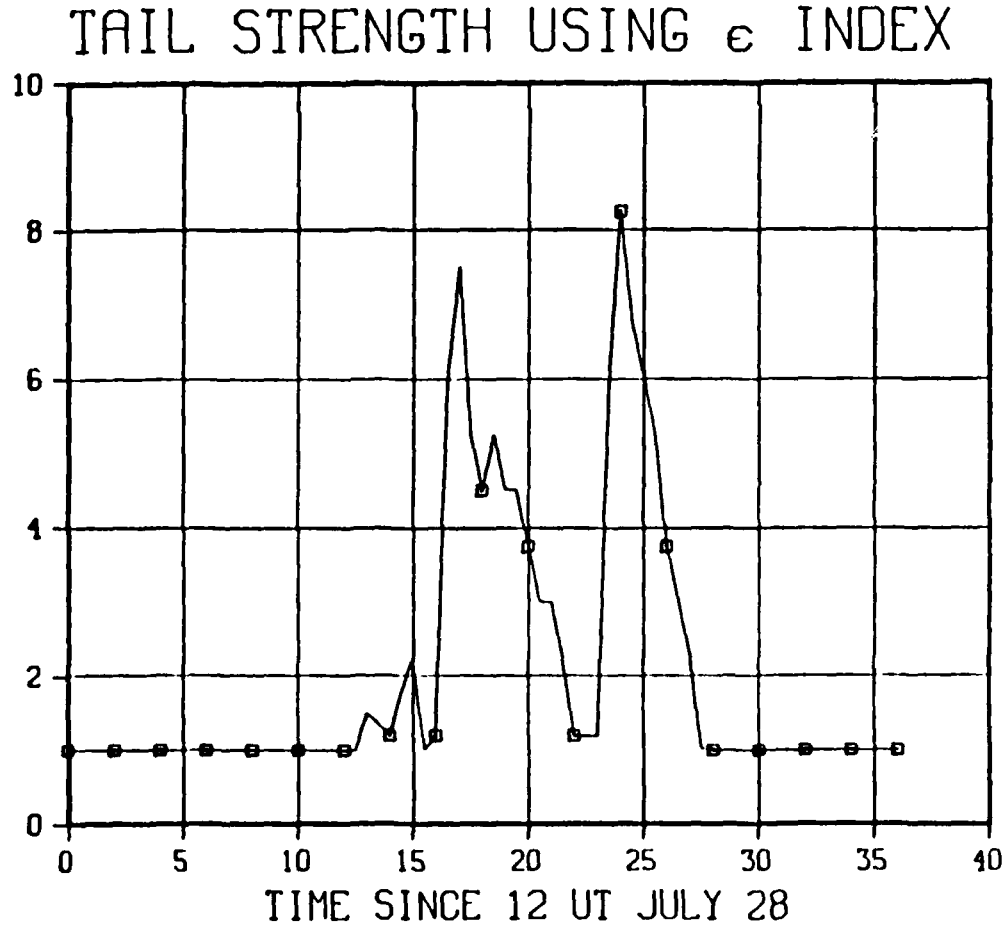

Figure 8. Tail Strength using ε Index

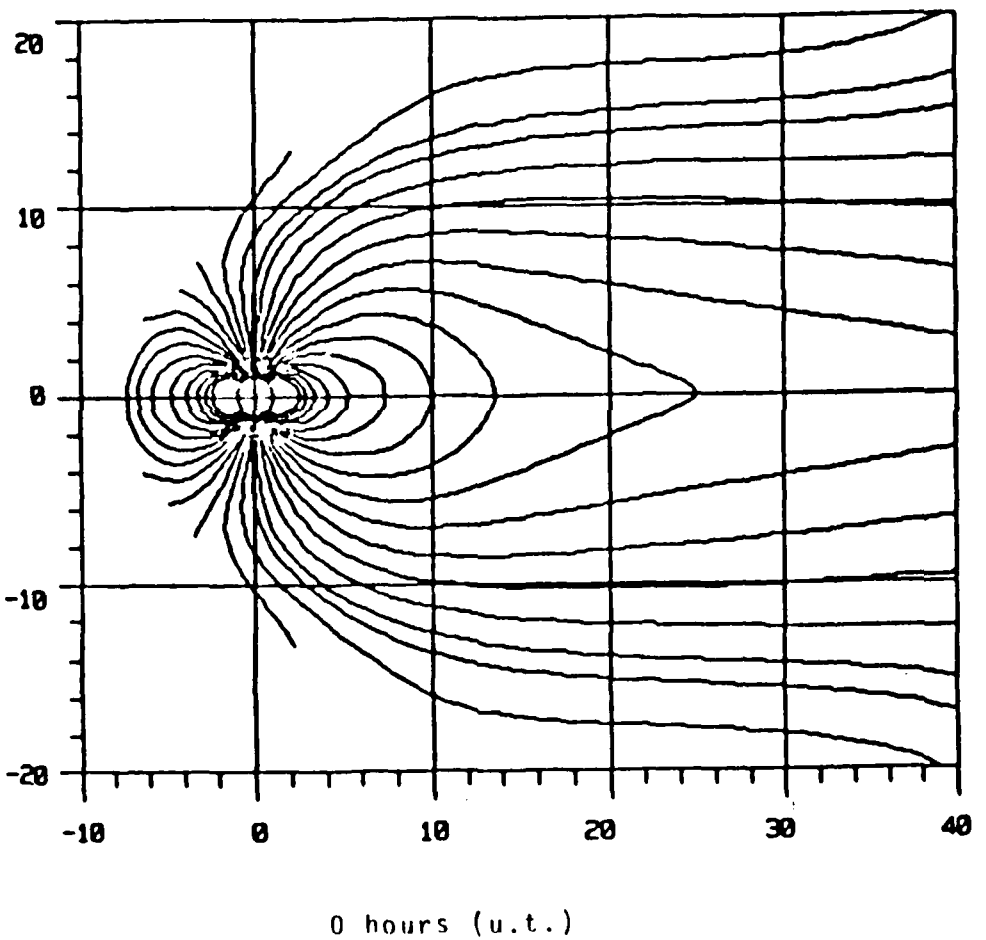

Figure 9. Magnetic Lines of Force in the Noon-Meridian Plane (0 hours)

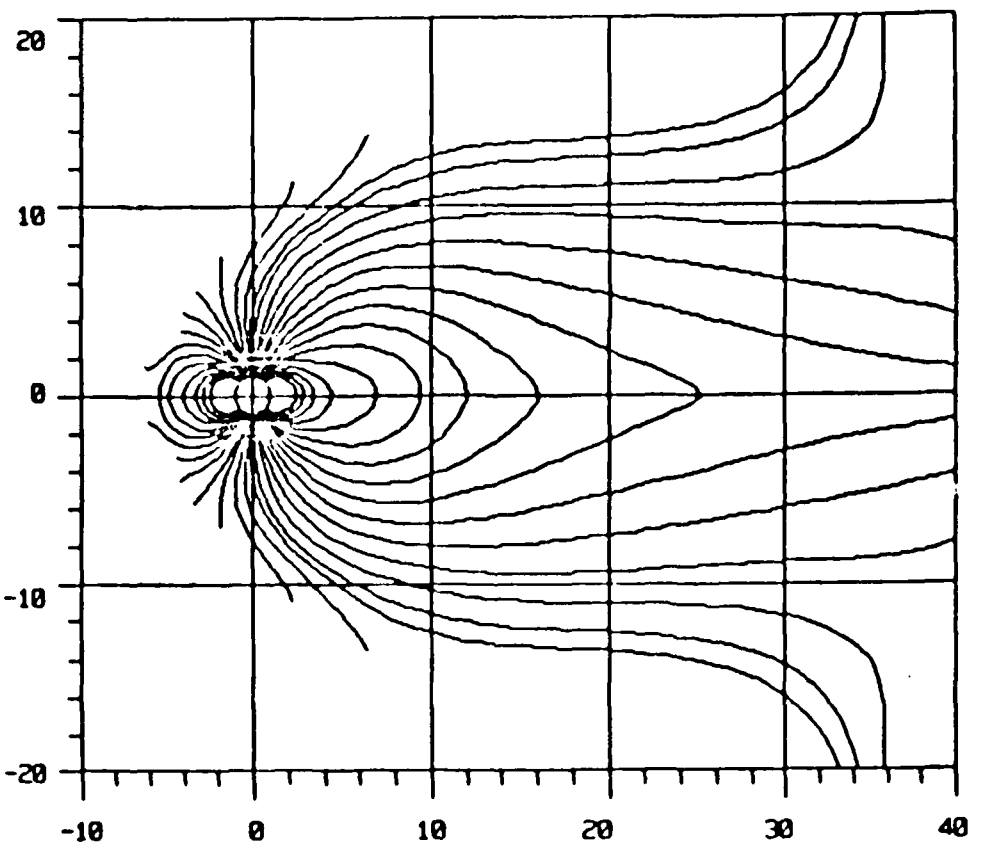

Figure 10. Magnetic Lines of Force in the Noon-Meridian Plane (4 hours)

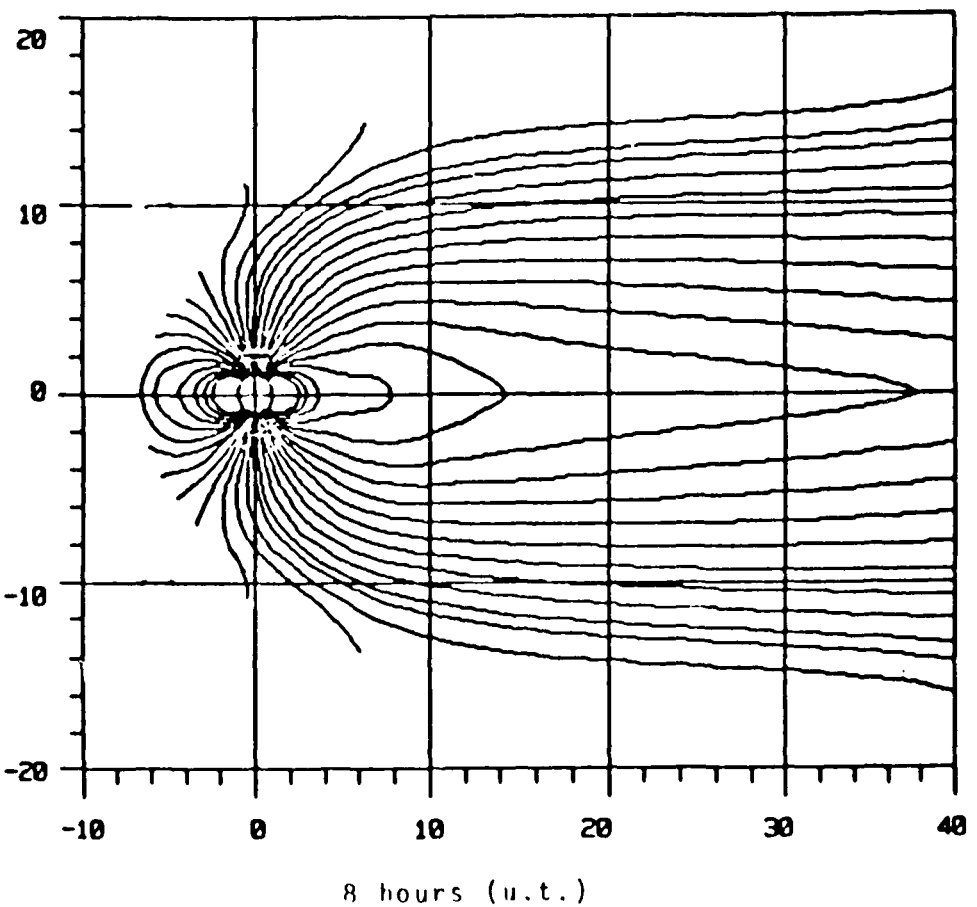

Figure 11. Magnetic Lines of Force in the Noon-Meridian Plane (8 hours)

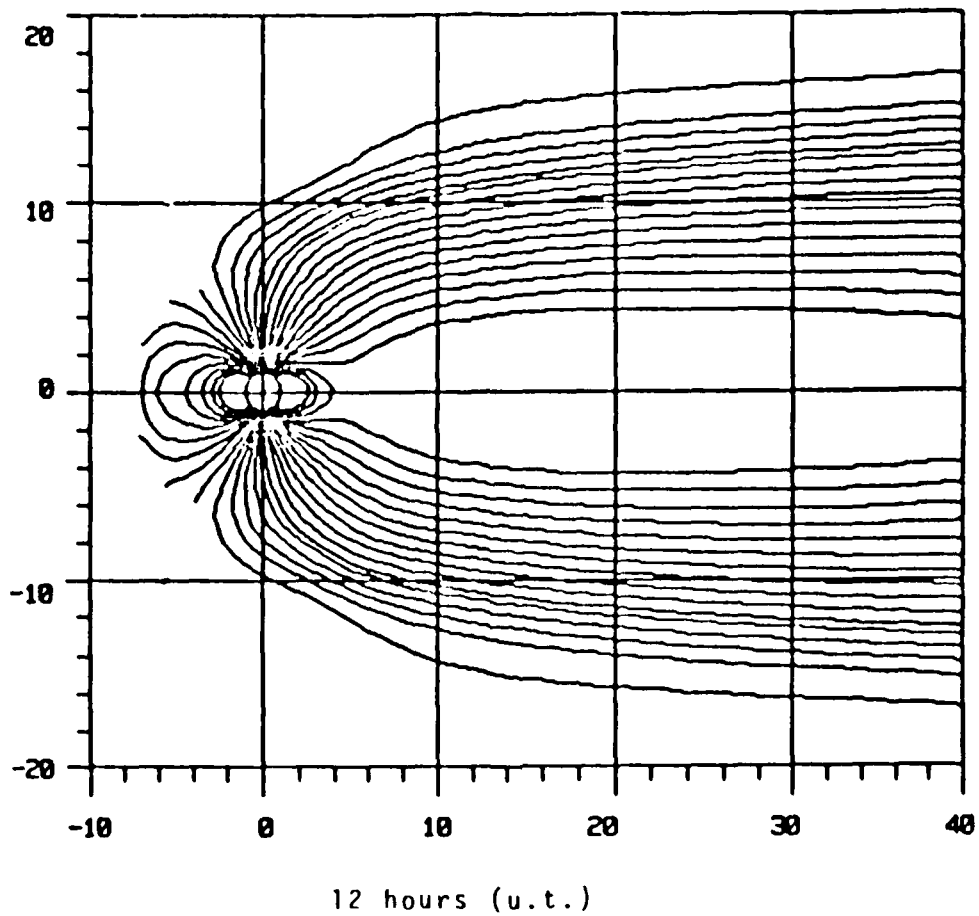

Figure 12. Magnetic Lines of Force in the Noon-Meridian Plane (12 hours)

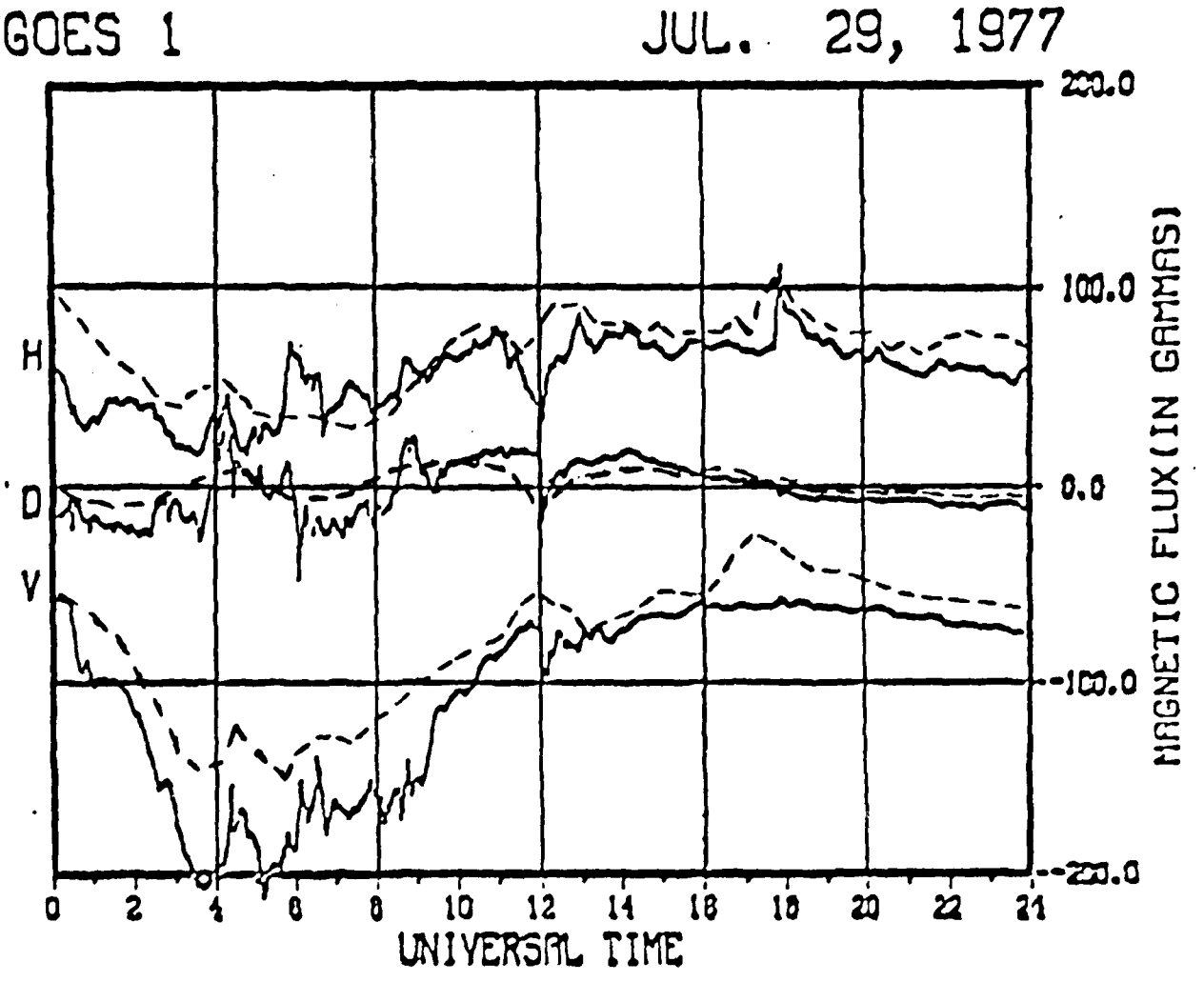

Figure 13. Comparison of the observed magnetic field at synchronous orbit (light variable line) with old non-disturbed model (light smooth line) and the new disturbed model (heavy line)

substorm structure observed is, indeed, included in the event model data. Also, it is not expected that the fit would be perfect, since the model input data were based on hourly or one-half hour averages.

The foot of the magnetic field line passing through the GOES 1 satellite at the ground in the northern hemisphere is shown in Figure 14 with a dashed line illustrating the track of the field line in a quiet model. The solid line shows the footprint during the event. Note that the line does not return to its starting point after 24 hours. Also, the large variability in foot location is of interest. In the past, 100 or 200 kilometers was considered the maximum for the daily excursion of the foot of the field line. Here, it is seen that the location varies by almost 1000 kilometers during this moderately disturbed period.

3.2 INDUCED ELECTRIC FIELD

It is convenient mathematically to work with the magnetic vector potential $\overline{A}$. In all of our recent modeling efforts we have routinely determined $\overline{A}$ when we calculate the magnetic induction $\overline{B}$. $\overline{A}$ is found much the same way as $\overline{B}$ by integrating over the current system according to the formula $\overline{A} = \mu_0/4\pi \int J dV/r$. It can be used directly to determine $\overline{B}$, from $\overline{B} = \nabla \times \overline{A}$. This is required in cases where $\nabla \cdot \overline{B}$ must be rigorously zero. (Our usual magnetic model consists of a direct representation of $\overline{B}$ and avoids the determination of $\nabla \times \overline{A}$, an additional numerical complication.) Also, the time variation in $\overline{A}$ directly yields the induced electric field, $-\partial \overline{A}/\partial t = \overline{E}_I$. Since the magnetospheric current system model includes the appropriate dependence on time (for the particular event under consideration), the time dependence of the magnetic field and the associated vector potential are also properly modeled. The induced component of the magnetospheric electric field resulting from this dependence of the magnetic field can be obtained from the vector potential.

$$\overline{E}_I = - \frac{\partial \overline{A}}{\partial t}$$

An example of $\overline{E}_I$ for the July 29 event is shown in Figure 15.

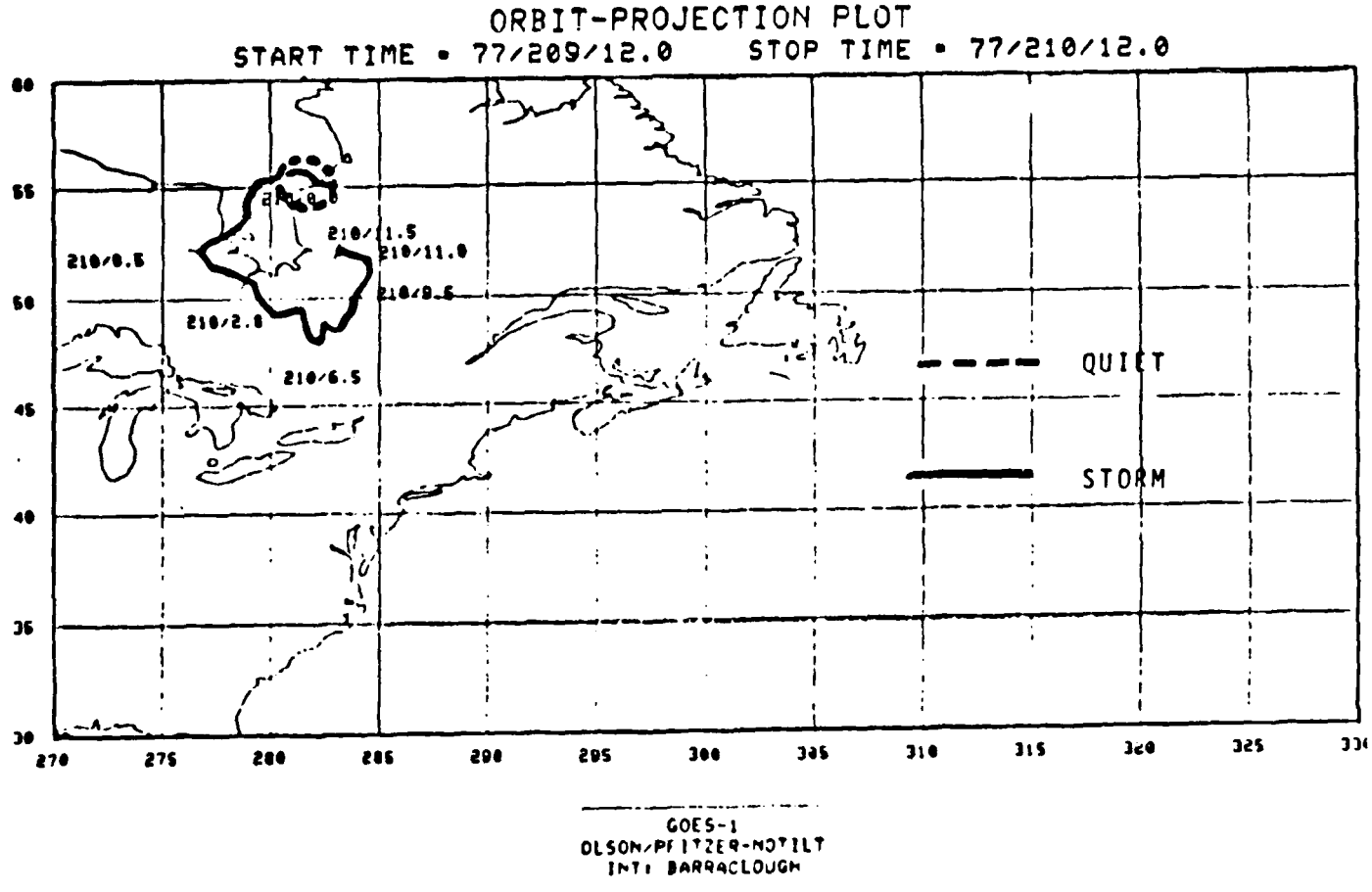

Figure 14. Footprint of the field lines from the synchronous orbit satellite GOES 1 as a function of universal time. (Numbers next to the footpoint track are day of year/universal time)

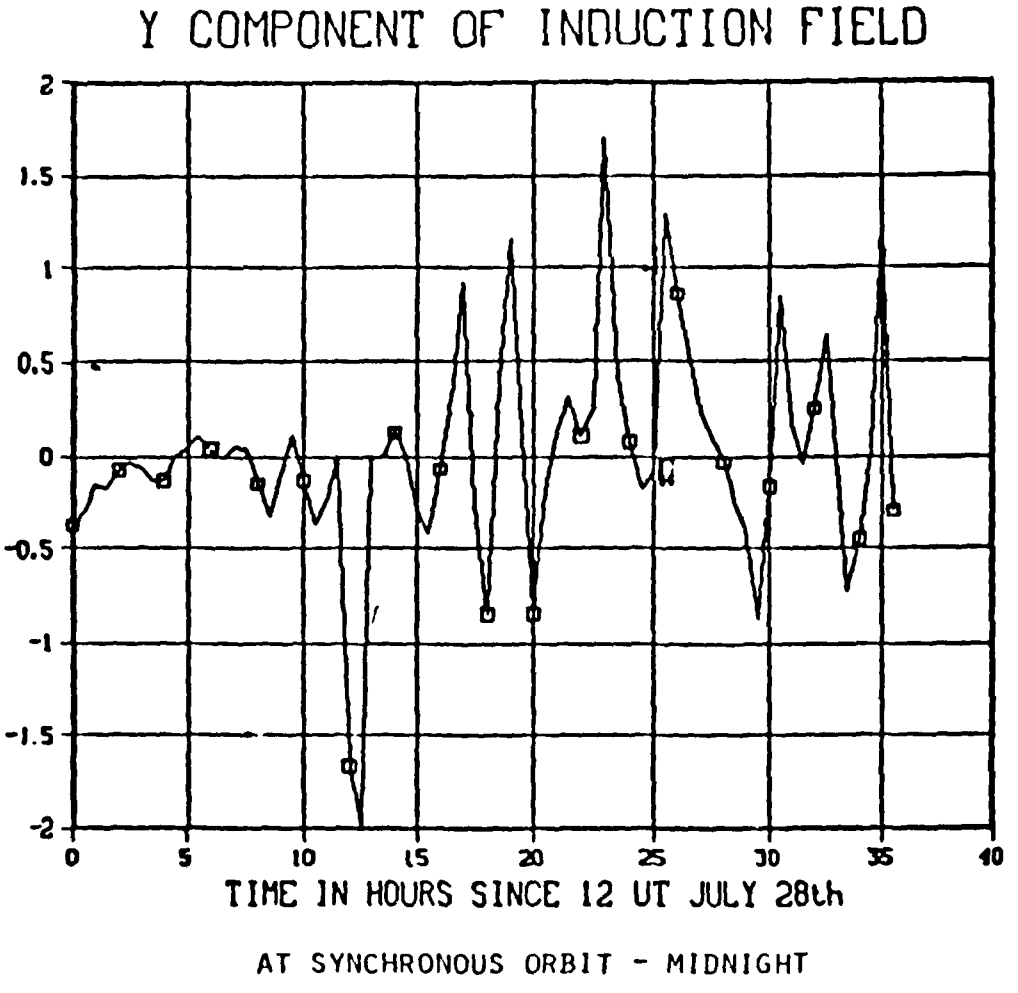

Figure 15. Y Component of Induction Field

However, because of the presence of charged particles (low density plasma) throughout the magnetosphere (this medium is the source of the current systems), local electric fields resulting from this medium must also be considered.

3.2.1 The Total Electric Field

Indeed, the total electric field at a given location will not only include the contribution from the local time dependence of the magnetic field, but also contributions from other regions of the magnetosphere transmitted to this location by the medium, to the extent that it is conductive. Thus, the total electric field,

$$\bar{E}_T = -\nabla\phi - \frac{\partial \bar{A}}{\partial t} \quad ,$$

at a given point in the magnetosphere includes contributions from the induced field from other regions of the magnetosphere, linked to the given location by the conductivity of the medium, as well as any contributions from local charge separation in the medium. This dependence is contained in the scalar potential component, $\bar{E}_S = -\nabla\phi$ of the total field.

A procedure developed by Hones and Bergeson (1965) was applied to evaluate the scalar potential component of the electric field. It is assumed that in the regions of interest, charged particle densities are high enough to assure sufficient conductivities along the magnetic field lines such that $\bar{E}_T \cdot \bar{B} = 0$.

Then

$$\frac{d\phi}{ds} = -\frac{\partial A_{\parallel}}{\partial t}$$

where $d\phi/ds$ is the scalar potential gradient along the field line, and $\partial A_{\parallel}/\partial t$ is the component of $\bar{E}_I$ parallel to the magnetic field line. This equation can be integrated along the field line to give the scalar potential at a given point in the magnetosphere. Thus,

$$\phi(r) = \phi_B - \frac{\partial}{\partial t} \int_{FL} \bar{A} \cdot d\bar{s}$$

where the line integral is along the field line, and ϕ_B is the potential at some appropriate boundary .

In the modeling of a realistic total electric field, care must be taken in the selection of the proper boundary condition as well as the value of $\partial A_{\parallel}/\partial t$ to be used in the integral. The presence of the medium complicates matters and careful estimates of the charged particle densities along the integration path must be made. If conductivities along the field line are sufficiently high, the induced electric field will propagate through very short distances and only local contributions of $\bar{E}_I$ will be significant. At lower densities, the integral may be extended along the magnetic field lines but then the question of the appropriate boundary condition must be considered. The various options available for the selection of $\partial A_{\parallel}/\partial t$ are summarized in Table 3-1.

The simple case of time independent $\bar{B}$ is included here only for completeness. It is consistent, however, with the assumption of magnetic field lines being equipotentials in an ionized medium. The second case represents the Hones and Bergeson procedure (discussed above) which is appropriate in regions where the conductivity along field lines is high enough so that $\bar{E} \cdot \bar{B} = 0$. The principal questions in applying this procedure is the selection of an appropriate boundary condition and the sources of magnetic field wihch contribute to $\partial A_{\parallel}/\partial t$. In the limit of very high conductivities, $\partial A_{\parallel}/\partial t$ approaches zero through energy dissipation, and only local sources of the magnetic field contribute. Case 3 illustrates this condition; again the magnetic field lines will either approximate equipotentials or only local sources of $\partial A_{\parallel}/\partial t$ will contribute to $\bar{E}$ parallel to the magnetic field line.

Case 4 in Table 3-1, represents the conditions present in areas where the conductivity along field lines is so low $\bar{E} \cdot \bar{B} \neq 0$. The procedures discussed in this report are not appropriate for this case and the only available approach is the solution of the wave equation. This can be done if a particularly convenient boundary condition for the regions of interest are available.

Table 3-1

VALUE OF $\frac{\partial A_{\parallel}}{\partial t}$

1. $\frac{\partial \bar{A}_{total}}{\partial t} = 0$: $\bar{E}_{total} = -\nabla\phi$ (time independent $\bar{B}$)

2. $\frac{\partial \bar{A}_{\parallel}}{\partial t} \neq 0$: if $\bar{E}\cdot\bar{B} = 0$ then $\frac{d\phi}{ds} = \frac{\partial A_{\parallel}}{\partial t}$ (Hones and Bergeson; Ionized Media Assumed)

3. $\frac{\partial A_{\parallel}}{\partial t} \sim 0$: by energy dissipation

   A. $d\phi/ds = \partial A_{\parallel}/\partial t \mid$ local

   B. $d\phi/ds \sim 0$ due to high conductivity

4. $\frac{\partial A_{\parallel}}{\partial t} \neq 0$: if $\bar{E}\cdot\bar{B} \neq 0$, then $d\phi/ds = ?$

Options for the selection of the appropriate boundary condition for ϕ include the following:

1. Experimentally determined.

2. Constant over an appropriate surface.

3. Uniformally magnetized rotating sphere (Hones and Bergeson, 1965),

   $V = \bar{U}\cdot\bar{A}$,

   V = the potential at point $\bar{r}$,

   $\bar{U} = \bar{w} \times \bar{r}$,

   $\bar{A} = \bar{\mu} \times \bar{r}/R_s^3$,

   $\bar{w}$ = angular velocity

   $\bar{\mu}$ = magnetic moment

   R_s = radius of sphere

4. A self-consistent rigorous determination of ϕ and $\bar{A}$.

In our work on the July 29 event, option 2 was used to evaluate $\bar{E}$ total.

3.2.2 Computational Difficulties

One of the big difficulties with the determination of the total Electric field $\bar{E}_I$ is the amount of computer time required. $\partial\bar{A}/\partial t$ is a series representation and can be directly evaluated at a point. However, $\nabla\phi$ requires the evaluation of three line integrals from the point and nearby points to the boundary surface and thus is computationally expensive. In order to study particle accelleration, particle trajectories or guiding center paths must be integrated over time. Thus the computational requirements become severe.

We are examining several approaches in an effort to reduce this computational requirement. Given a fixed boundary condition and a specific time history for $\partial\bar{A}/\partial t$, a specific time dependent function can be generated for $\nabla\phi$. A second method for solving this specific problem using Euler potentials is discussed in the appendix. Both of these techniques require the definition of a specific time dependent history for the magnetic field and $\bar{E}_I$ and the boundary condition. Changing either of these conditions will require a complete recalculation of $\nabla\phi$. The technique should, however, be useful in the study of a classical event and the accompanying particle motions and accellerations.

Section 4.0

RESULTS AND CONCLUSIONS

The study of event specific storm time magnetospheric fields has led to several intersecting results and conclusions including the following:

- Although $\overline{E}_T$ was not determined routinely because of computer time problems, enough "data" were obtained to illustrate qualitatively that E_I from $\partial B/\partial t$ can cause the local acceleration of charged particles observed during the July 29 event.

- The value of $\overline{E}_T$ ($= \overline{E}_I + \overline{E}_S$) is very dependent on the scalar potential of the electric field on the ionosphere. Thus, the accurate determination of $\overline{E}_T$ for a given event requires not only a knowledge of $\overline{B}/(t)$ but also the variations in ϕ_B. This implies that the ionosphere exerts considerable influence on magnetospheric fields and low energy plasma.

- Although STARE data were available (they could be used to make a comparison between the $\overline{E}$ field in the ionosphere and at satellite altitudes) no study was performed since the validity of the satellite electric field data has become questionable. (The electron gun and double probe experiments on GEOS-1 have yielded significantly different results - suggesting problems with the double probe method.)

- Because of the problem of computer time we have not yet attempted to quantitatively study the behavior of charged particles in these electromagnetic field environments. The possible use of Euler potentials as a time saving device is being investigated and is discussed in some detail in the Appendix.

- The work described here represents the first attempt to quantitatively model a specific magnetospheric event. We feel it was quite successful.

- We feel that our procedures for representing electric fields in the magnetosphere produced by time variations in the magnetic field (and the response of the magnetospheric plasma to such electric fields) are correct, complete - and complex. It remains to quantitatively represent the electrostatic field in the tail of the magnetosphere. Our ideas on this subject have been proposed to your office.

Appendix

USING EULER POTENTIALS IN FIELD MODELS

Generally the electric field is given by the equation

$$\bar{E} = -\frac{1}{c}\frac{\partial \bar{A}}{\partial t} - \nabla\phi \qquad (1)$$

The difficulty with the electric field models we have derived thus far is that in determining the total electric field at a given point p, it is necessary to numerically integrate down the field line through p to its earth intercept in order to determine the electrostatic potential ϕ at p. This procedure must be followed for several points near p so that a finite difference analog to $\nabla\phi$ can be obtained (the $\partial\bar{A}/\partial t$ part of $\bar{E}$ is determined point-wise). Thus, solving for the motion of a single trapped particle under the influence of the electric and magnetic fields requires an enormous amount of computer time because the integrals for $\nabla\phi$ must be computed at each time step.

The problem is not how do we compute the electromagnetic fields that influence particle motion, but how do we solve the problem of particle motion economically. The solution involves recasting our magnetic and electric field models so that the $\nabla\phi$ term in (1) is effectively changed from an integral to a point-wise function. The method discussed here is to use an Euler potential representation of the magnetic field.

Euler Potentials

The properties of Euler potentials are listed and/or derived in several places (1, 2, 3, 4, 5, 6, 7). Essentially, these potentials, usually defined as α and β, are such that they are constant on a field line and the relations

$$\bar{B} = \nabla\alpha \times \nabla\beta \qquad (2)$$

$$\bar{A} = \alpha\nabla\beta + \nabla\tau$$

where $\nabla\tau$ is the gauge, are satisfied. There are an infinite set of (α,β) that satisfy these relations and any other pair of potentials (α',β') can be derived

from a given pair (α,β) by a time-dependent transformation of the given pair such that the Jacobian of the transformation is unity. This non-uniqueness is equivalent to a gauge transformation of the vector $\bar{A}$ [5], and the arbitrary time dependence makes it impossible to define the field line velocity (from conservation of α and β with field line motion) without other physical constraints [2].

Neglecting the gauge contribution to $\bar{A}$, the electric field expressed in terms of these potentials is

$$\bar{E} = -\frac{1}{c}\frac{\partial}{\partial t}(\alpha\nabla\beta) - \nabla\phi \tag{3}$$

$$= -\frac{\bar{W}\times\bar{B}}{c} - \nabla(\phi+\psi)$$

where

$$\bar{W} = \left(\frac{\partial\beta}{\partial t}\nabla\alpha - \frac{\partial\alpha}{\partial t}\nabla\beta\right)\times\bar{B}/B^2$$

and

$$\psi = \frac{1}{c}\alpha\frac{\partial\beta}{\partial t}$$

Using the assumption that $\bar{E}\cdot\bar{B} = 0$, we see that the quantity $\phi + \psi$ is constant along a field line. Assuming that the earth boundary is a rotating and translating, perfectly conducting, magnitized sphere, if we choose α and β so that they are constant at a given geographic position on the sphere; then we can derive, as in [5], that $\phi + \psi$ is constant everywhere. Then $\bar{W}$ is the actual field line velocity as defined by the $\bar{E}\times\bar{B}$ drift. For more general boundary conditions on ϕ, the field lines will "slip" and not be anchored to fixed position in the ionosphere. The Euler potentials are then not so easily chosen so that $\bar{W}$ will define the field line velocity; however, this is of no concern in charged particle energization problems. Since the different choices of Euler potentials corresponds to different choices of gauge for $\bar{A}$, and since charged particle energization is gauge invariant [6]; we can choose a set of Euler potentials that is the most convenient to use.

Development of an Euler Potential Model

We will now describe the steps necessary to construct a Euler potential model from an existing external magnetic field model and a dipole internal field. One disadvantage of using Euler potentials is that they are non-linear and must be derived from the full field representation of $\bar{B}$. We will use the solar magnetospheric coordinate system (herein called "SM', it has unit vectors $\hat{i}_x$, $\hat{i}_y$, $\hat{i}_z$ and corresponding coordinates XSM, YSM, ZSM) to develop the Euler potentials.

The simplest pair of Euler potentials, that is approximately correct very close to the earth, is due to the dipole

$$\alpha_d = a\, g_1^0 \left(\frac{a}{|\bar{r}|}\right) \sin^2 \theta \qquad (4)$$

$$\beta_d = a\, \lambda$$

where θ is the angle between the north dipole axis and the observation point $\bar{r}$ ($\cos\theta = \hat{i}_{dp} \cdot \bar{r}/|\bar{r}|$; $\hat{i}_{dp}$ is the unit north pointing dipole vector), λ is the azimuth angle about the dipole axis with λ increasing counter-clockwise about the axis ($\lambda = 0$ corresponds to the XSM-ZSM plane and λ can be found from

$$\bar{r} = R_\perp[\hat{i}_{dp} \times \hat{i}_y) \cos\lambda + \hat{i}_y \sin\lambda] + R_{||}\, \hat{i}_{dp},)$$

a is the earth's radius, and g_1^0 is the dipole moment in units of gauss or gammas.

To find the distribution of (α,β) in space, we choose a grid of points on earth's surface ($|\bar{r}| = a$) whose field lines intersect the region of space in which we wish to model the fields. We then march up the field lines using the dipole field plus the external field representation for $\bar{B}$ to determine the direction of marching. We assign the boundary values of α and β minus (α_d, β_d) to each point of the field line - call this set (α^*,β^*). This procedure is followed for all the grid points at a number of "tilt" angles (of the dipole with respect to the ZSM axis) or in the storm case for a number of different time steps. The resultant set (α^*,β^*) will be a function of

XSM, YSM, ZSM and tilt angle. Note that there will be a number of symmetries that can be utilized to reduce the number of points needed because of the assumed dipole internal field (i.e., only positive tile angles needed, symmetry of field line across the XSM-ZSM plane). The set (α^*,β^*) is then curvefit such that the fit goes to zero at $|\bar{r}| = a$. This device ensures that we recover the simple analytic representation of the potentials as we approach the earth; and also that the assumption of (4) (which is only approximate near the earth) will not introduce ambiguities in the definition of α and β at the conjugate points of a field line. Setting $(\alpha,\beta) = (\alpha_d,\beta_d) + (\alpha^*,\beta^*)$, we will have a set of Euler potentials which we can use to investigate charged particle energization.

Use of the Euler Potential Model to Find $\bar{E}$ and $\bar{B}$

The simplest way to describe charged particle motion is to use the guiding center equations in an inertial reference frame (X, Y, Z). A coordinate transformation exists between the SM system and the inertial system which is essentially a time dependent rotation if the same origin is used. (α,β) transform as scalars between the two systems; so we can compute the $\bar{B}$ or $\bar{A}$ fields either by 1) setting up finite difference points in the inertial system, transforming them to the SM system, finding (α,β), and forming the gradient analog in the inertial system; or 2) transforming the point for gradient evaluation to SM coordinates, finding the gradient at this point, and transforming the gradient vector to the inertial system. The second approach is more attractive, especially if the gradients of α and β can be given analytically in the SM system.

To find the $\bar{E}$ field in the inertial system, we will need to evaluate (3). One method to use is:
1) Given a point (X, Y, Z) at time t, transform to the SM system and determine α, β, and $\nabla\beta$; transform $\nabla\beta$ to the inertial system. Do the same at time $t + \delta t$. By finite differences, we can form the $\partial\bar{A}/\partial t$ contribution to (3).
2) Find the position on the earth's surface that has the same (α,β) values from (4). Take the boundary value of ϕ defined at this point. 3) Using the condition that $\bar{E} \cdot \bar{B} = 0$, we have $\phi + \psi = C$, a constant along the field line defined by constant (α,β). ψ in the inertial system is given by $1/c\ \alpha\ \partial\beta/\partial t|_{X,Y,Z}$ so it is possible to define ψ on the earth's surface

analytically using (4) which is time dependent in the SM system, and the time dependent coordinate transformation from the SM system to the inertial system. C is determined from the values of ϕ and ψ on the earth's surface. 4) We can form ψ at (X,Y,Z) by a finite difference in time and find ϕ by $\phi = C - \psi$. 5) By repeating the preceding steps (except for finding $\nabla\beta$) for points around (X,Y,Z), we can form a finite difference analog for $\nabla\phi$ in the inertial system.

Using the above procedure, the total electric field due to the wobbling dipole and the boundary condition on ϕ can be found. The need to integrate along field lines to find is removed since this was done when we modeled the Euler potentials. Note that the constraint $\phi + \psi = C$ on a field line makes it necessary to define the boundary only on one side of the geomagnetic equator. The $\overline{E}$ and $\overline{B}$ fields can be used with the equations of guiding center motion (such as in [7]) to investigate the effects of the magnetic and electric fields on charged particle energization quantitatively.

REFERENCES

[1] Stern, D. P., Representation of Magnetic Fields in Space, Rev. Geophys. Space Phys., 14, 199, 1976.

[2] Stern, D. P., An Inverse Theorem About the Magnetic Field Line Velocity, J. Geophys. Res., 78, 1702, 1973.

[3] Stern, D. P., Euler Potentials, Amer. J. Phys., 38, 494, 1970.

[4] Stern, D. P., The Motion of Magnetic Field Lines, Space Sci. Rev., 6, 147, 1966.

[5] Birmingham, T. J. and F. C. Jones, Identification of Moving Magnetic Field Lines, J. Geophys. Res., 73, 5505, 1968.

[6] Birmingham, T. J. and T. G. Northrop, Charged Particle Energization by an Arbitrarily Moving Magnet, J. Geophys. Res., 73, 83, 1968.

[7] Northrop, T. G, The Adiabatic Motion of Charged Particles, John Wiley and Sons (Interscience), New York, 1963.

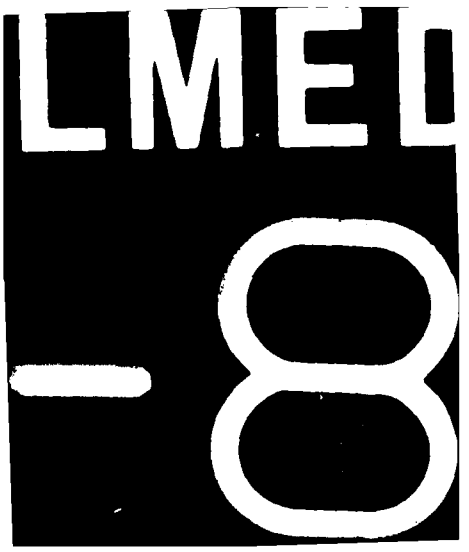
LMEL
-8